Colloid Polym Sci (2009) 287:403–412
DOI 10.1007/s00396-008-1977-9

ORIGINAL CONTRIBUTION

The electrorheological efficiency of polyaniline particles with various conductivities suspended in silicone oil

Martin Stěnička · Vladimír Pavlínek · Petr Sáha · Natalia V. Blinova · Jaroslav Stejskal · Otakar Quadrat

Received: 8 September 2008 / Revised: 26 November 2008 / Accepted: 28 November 2008 / Published online: 18 December 2008

Abstract Electrorheological (ER) behavior of silicone oil suspensions of particles of polyaniline protonated to various doping levels with *ortho*-phosphoric and tetrafluoroboric acids has been studied. The dynamic yield stress obtained by extrapolation of shear stress to zero shear rate using Herschel–Bulkley equation was used as a criterion of the ER efficiency. At a same molar concentration of doping acids, various protonation effects appeared and the dependences of the yield stress on the acid concentration differed. The comparison of the yield stresses with dielectric characteristics calculated from the Havriliak–Negami equation revealed that the particle conductivity, in contrast to particle permittivity, dominates the polarization process especially at higher protonation degrees. Consequently, particle conductivity or dielectric relaxation time proved to be the parameters providing the common dependences of the yield stress regardless of the way of polarization.

Keywords Electrorheology · Suspension · Yield stress · Conductivity · Relaxation time · Polyaniline

Introduction

Electrorheological (ER) fluids, composed of semiconducting particles dispersed in non-conducting liquids, are intelligent materials whose structure and rheological properties are quickly and reversibly changed under application of external electric field with the strength of several kilovolts per millimeter. This effect occurs due to particle polarization and consequent formation of a chain-like or columnar structure-oriented parallel to stream lines of the electric field. Consequently, the rigidity of these structures increases and, when a shear force is applied, the viscosity at low shear rates is much higher than that in the absence of the electric field. In some cases at rest, quasi-gel materials with a high yield stress may arise. When the electric field is switched off, the suspension returns to its original state.

Since the pioneering discovery of the ER phenomenon by Winslow [1], a number of studies of its mechanism have been carried out. The main results have been summarized in several reviews [2–8]. The potential applications of such smart materials have stimulated a great deal of interest in both academic and industrial areas. Vibration damping devices (dampers of engine mounts), force transfers such as clutches and valves, brakes, and other hydraulic systems or micro-robotics [9] are among the typical applications of practical significance.

Considerable attention of research teams conversant with ER effect is presently focused on findings of the most suitable ER suspension, which enable the enhancement of ER efficiency. The application of a group of semiconducting polymers, represented by polyaniline (PANI) [10–13], polypyrrole [14], or polyphenylene [15, 16], appears as a possible trend because of the high ability of polymer particles to be polarized. Conductivity of these polymers is given by the chemical structure of polymer chains comprising π-bonds that alternate with σ-bonds and form a conjugated system. Electric and dielectric properties of these materials affecting particle polarizability of PANI can be controlled via the protonation with various acids [17–20]. The different acids can also affect its structure

M. Stěnička · V. Pavlínek (✉) · P. Sáha
Faculty of Technology, Tomas Bata University in Zlín,
TGM Sq. 275, 762 72,
Zlín, Czech Republic
e-mail: pavlinek@ft.utb.cz

N. V. Blinova · J. Stejskal · O. Quadrat
Institute of Macromolecular Chemistry,
Academy of Sciences of the Czech Republic,
Heyrovsky Sq. 2, 162 06,
Prague, Czech Republic

Table 1 The density ρ, conductivity σ, relative permittivity $\varepsilon'_{p,0}$, and particle dipole coefficient β (see Eq. 6) of PANI base reprotonated in the aqueous solutions of *ortho*-phosphoric acid of various molar concentrations C_A

Sample	C_A (mol l^{-1})	ρ (g cm^{-3})	σ (S cm^{-1})	$\varepsilon'_{p,0}$	β
B	0	1.132	3.6×10^{-9}	26.0	0.750
P1	0.0001	1.144	4.7×10^{-9}	26.1	0.752
P2	0.0005	1.114	6.8×10^{-9}	27.8	0.755
P3	0.001	1.112	2.7×10^{-8}	30.2	0.767
P4	0.005	1.145	5.8×10^{-7}	31.7	0.769
P5	0.01	1.264	4.7×10^{-5}	35.7	0.792
P6	0.05	1.333	3.1×10^{-3}	41.1	0.805

and degree of crystallinity [21]. It is clear that doping offers a simple tool to gain materials with optimum conductivity and permittivity for the maximum ER performance.

Compared to similar semiconducting polymers, PANI has several advantages such as simple preparation, easy conductivity control, good thermal and environmental stability as well as a favorable production cost. Consequently, investigation of its preparation and properties has attracted significant attention in the last three decades [22].

In our previous work [23], we focused our attention on the investigation of the time dependences of conductivities of the suspensions of the series of PANI samples protonated by *ortho*-phosphoric acid to various levels during the formation of chain-like structures in the DC electric field. The increase in conductivity reflects the formation of ER structure. In addition, the influence of the flow field on this process was examined in detail. The comparison of the ER efficiency of PANI powders protonated by *ortho*-phosphoric or tetrafluoroboric acids [24] with a different protonation effect was the object of the current study. The dynamic yield stress of silicone oil suspensions was applied as a suitable tool for evaluation of strengthening of the particle structure in the electric field.

Table 2 The density ρ, conductivity σ, relative permittivity $\varepsilon'_{p,0}$, and particle dipole coefficient β (see Eq. 6) of PANI base reprotonated in the aqueous solutions of tetrafluoroboric acid of various molar concentrations C_A

Sample	C_A (mol l^{-1})	ρ (g cm^{-3})	σ (S cm^{-1})	$\varepsilon'_{p,0}$	β
B	0	1.132	3.6×10^{-9}	26.0	0.750
T1	0.0001	1.149	4.9×10^{-9}	26.2	0.752
T2	0.0005	1.154	4.9×10^{-9}	26.7	0.755
T3	0.001	1.142	9.0×10^{-9}	28.3	0.767
T4	0.005	1.163	1.6×10^{-8}	28.6	0.769
T5	0.01	1.157	1.2×10^{-5}	32.4	0.792
T6	0.05	1.168	2.5×10^{-4}	35.0	0.805

Experimental

Controlled protonation of PANI with ortho-phosphoric and tetrafluoroboric acids PANI powder was prepared by the oxidation of 0.2 M aniline hydrochloride with 0.25 M ammonium peroxydisulfate in water [25] at 20 °C; its conductivity was 4.4 S cm^{-1}. The obtained PANI salt was transformed into the PANI base by 2-day immersion in a fivefold molar excess of 1 M ammonium hydroxide (50 ml per 1 g of PANI salt), filtering of the precipitate, and drying in air. The conductivity of PANI base was 3.6×10^{-9} S cm^{-1}. Portions of the PANI base (0.5 g) were suspended in 100 ml of aqueous solutions of either *ortho*-phosphoric or tetrafluoroboric acid solutions of various acid concentrations for 24 h, separated, rinsed with acetone, and dried as above. Protonation degree of the samples was expressed by molar concentration C_A of the acid used. For pH values and the correlation between pH and conductivity, the reader is referred to Ref. [24]. The density of PANI was then determined by weighing compressed pellets on Sartorius R160P balance on air and immersed in decane.

Conductivity measurements The DC conductivity, σ, of protonated PANI samples pressed at 700 MPa into pellets 13 mm in diameter and 1 mm thickness was determined by a two-point method (at $\sigma<10^{-5}$ S cm^{-1}) (Keithley 6517 electrometer) or by four-point method at higher conductivities (a current source SMU Keithley 237 and a Multimeter Keithley 2010 voltmeter with a 2000 SCAN 10-channel scanner card) (Tables 1 and 2).

Suspension preparation PANI powders were ground using an agate mortar and pestle, sieved to obtain particle sizes smaller than 45 μm, and dried at 80 °C in a vacuum oven to a constant weight. Suspensions (10 wt.%) were prepared by mixing PANI powders with corresponding amount of silicone oil (Lukosiol M200, Chemical Works Kolín, Czech Republic, viscosity η_c=200 mPa s, density ρ_c=0.965 g cm^{-3}, conductivity $\sigma_c\approx10^{-11}$ S cm^{-1}, relative permittivity ε'_c=2.6, loss factor tan δ=0.002). At first, the samples were stirred mechanically and then placed in an ultrasonic bath for 30 s

Table 3 Parameters of H–N equation (Eq. 2) for *ortho*-phosphoric acid-doped PANI particles

Sample	$\varepsilon'_{s,0}$	$\varepsilon'_{s,\infty}$	t_{rel} (s)	a	b
B	4.62	2.66	1.48×10^{-2}	0.80	0.69
P1	4.62	2.66	1.16×10^{-2}	0.86	0.60
P2	4.82	2.67	9.88×10^{-3}	0.76	0.70
P3	5.03	2.70	5.23×10^{-3}	0.70	0.70
P4	5.10	2.65	1.27×10^{-3}	0.61	0.69
P5	5.19	2.60	8.27×10^{-6}	0.37	0.97
P6	5.47	2.64	3.33×10^{-7}	0.59	0.73

Table 4 Parameters of H–N equation (Eq. 2) for tetrafluoroboric acid-doped PANI particles

Sample	$\varepsilon'_{s,0}$	$\varepsilon'_{s,\infty}$	t_{rel} (s)	a	b
B	4.62	2.66	1.48×10^{-2}	0.80	0.69
T1	4.64	2.62	1.46×10^{-2}	0.84	0.65
T2	4.58	2.64	1.27×10^{-2}	0.81	0.67
T3	4.81	2.69	7.39×10^{-3}	0.73	0.74
T4	4.80	2.61	4.47×10^{-3}	0.63	0.90
T5	5.13	2.66	1.86×10^{-4}	0.54	0.78
T6	5.32	2.72	3.53×10^{-6}	0.50	1.00

before each measurement. In this study, only the PANI samples with conductivity up to 4.7×10^{-5} S cm^{-1} have been used because conductivity of the samples doped by a more concentrated acid was too high and, consequently, the strings of polarized particles short cut the circuit in the electric field and measurement of the ER effect was impossible. More conducting samples were used in our previous study [23].

Electrorheological measurements The ER properties were measured with a rotational rheometer Bohlin Gemini (Malvern Instruments, UK), with parallel plates 40 mm in diameter and a gap of 0.5 mm, modified for ER experiments. The measurement was carried out in the range of shear rates 1–100 s^{-1} (controlled shear rate mode). The chosen geometry was connected to a DC high-voltage source TREK (TREK 668B, USA) providing the electric field strength E=0.5–3.0 kV mm^{-1}. Before each measurement at new electric field strength, the built-up particulate structure was always destroyed by shearing of the sample at a shear rate of 20 s^{-1} for 80 s. The temperature during all the experiments was kept at 25 °C.

Dielectric measurements The frequency dependences of complex permittivity of 10 wt.% suspensions (Eq. 1):

$$\varepsilon^*_s = \varepsilon'_s(f) - i\varepsilon''_s(f) \tag{1}$$

involving the relative permittivity $\varepsilon'_s(f)$ and dielectric loss factor $\varepsilon''_s(f)$ were measured with a Hioki 3522 RCL HiTester (Japan) in the range $f=10^1$–10^5 Hz. The dielectric characteristics of particle suspensions (Tables 3 and 4) were obtained from the Havriliak–Negami (H–N) empirical model (Eq. 2) fitting by least square method [26]:

$$\varepsilon^*_s(f) = \varepsilon'_{s,\infty} + \frac{\left(\varepsilon'_{s,0} - \varepsilon'_{s,\infty}\right)}{\left(1 + (i\,2\pi f\, t_{rel})^a\right)^b} \tag{2}$$

Here, $\varepsilon^*_s(f)$ is a complex suspension permittivity and $\varepsilon'_{s,0}(f)$ and $\varepsilon'_{s,\infty}(f)$ are the limit values of the relative permittivity at the frequencies below and above the relaxation frequencies (see Figs. 3 and 4), f is a frequency, t_{rel} is a relaxation time (see Eq. 5), a is the scattering degree of relaxation times, and b is related to the asymmetry of the relaxation time spectrum. Large values of a mean a great scattering of relaxation times. When a differs significantly from zero and b significantly from unity, the relaxation spectrum becomes more asymmetrical.

The static relative particle permittivity $\varepsilon'_{p,0}$ (Tables 1 and 2) was estimated from the static relative permittivity of suspensions $\varepsilon'_{s,0}$ and permittivity of the continuum ε'_c using the volume-average equation (Eq. 3) [27]:

$$\varepsilon_{p,0} = \varepsilon'_c + \frac{\left(\varepsilon'_{s,0} - \varepsilon'_c\right)}{\xi} \tag{3}$$

where ξ is a volume fraction of the solids.

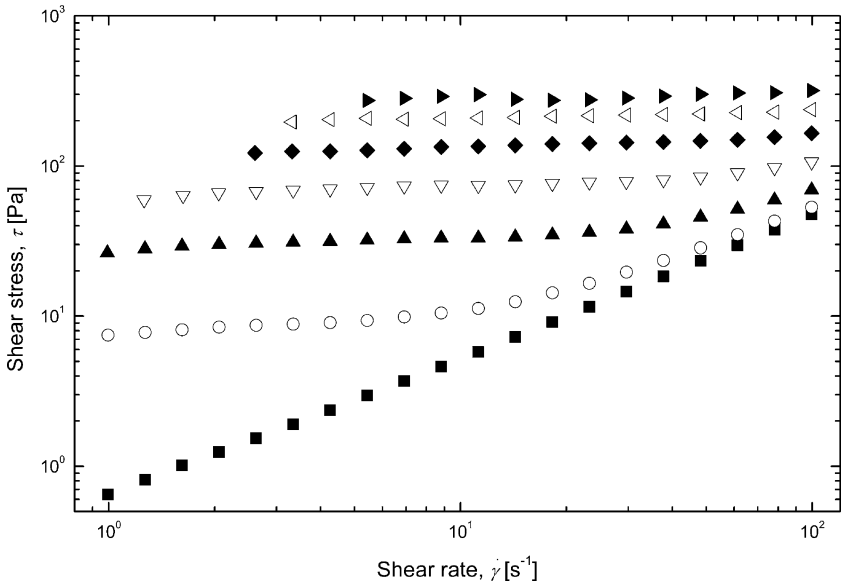

Fig. 1 Double-logarithmic plot of the shear stress τ vs. shear rate $\dot{\gamma}$ for the suspension of the sample P5 at various electric field strengths E (kV mm^{-1}): ■ 0, ○ 0.5, ▲ 1.0, ▽ 1.5, ♦ 2.0, ◁ 2.5, ▶ 3.0

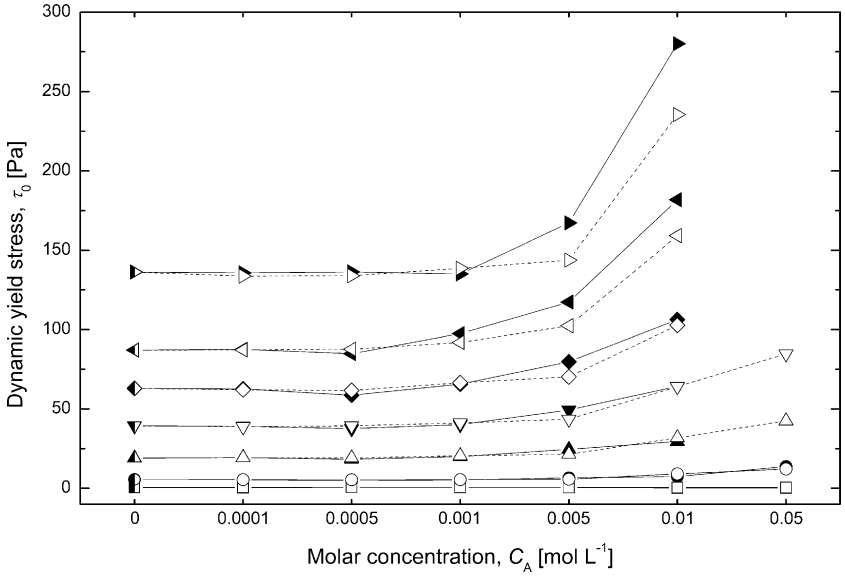

Fig. 2 The dependence of the dynamic yield stress τ_0 on the molar concentration of the acid C_A used for the reprotonation of PANI base at various electric field strengths. *Ortho*-phosphoric acid (*solid symbols*); tetrafluoroboric acid (*open symbols*); original PANI base (*divided symbols*). Electric-field strength E (kV mm^{-1}): ■□ 0, ●○ 0.5, ▲△ 1.0, ▼▽ 1.5, ♦◇ 2.0, ◀◁ 2.5, ▶▷ 3.0

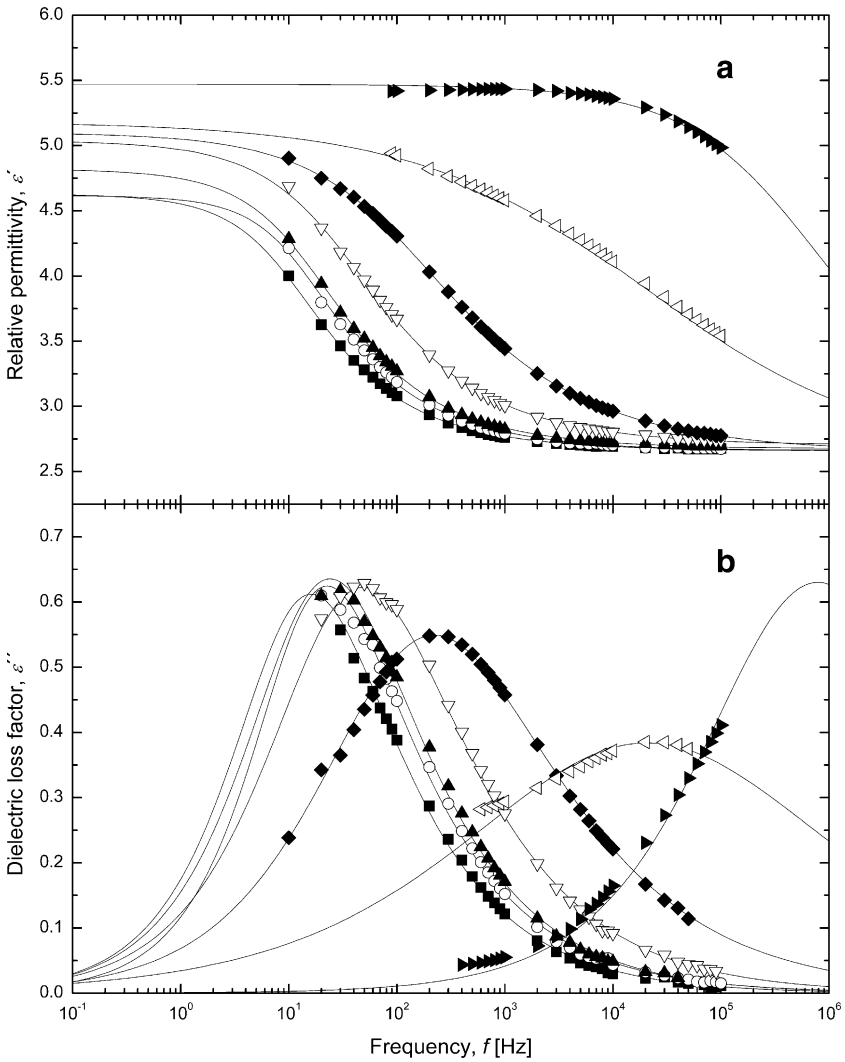

Fig. 3 Frequency spectra of relative permittivity ε' (**a**) and dielectric loss factor ε'' (**b**) for PANI suspensions protonated by *ortho*-phosphoric acid. Molar concentrations of acid C_A (mol l^{-1}) used for reprotonation of PANI base: ■ 0, ○ 0.0001, ▲ 0.0005, ▽ 0.001, ♦ 0.005, ◁ 0.01, ▶ 0.05. *Lines* are fits of the H–N model (Eq. 2)

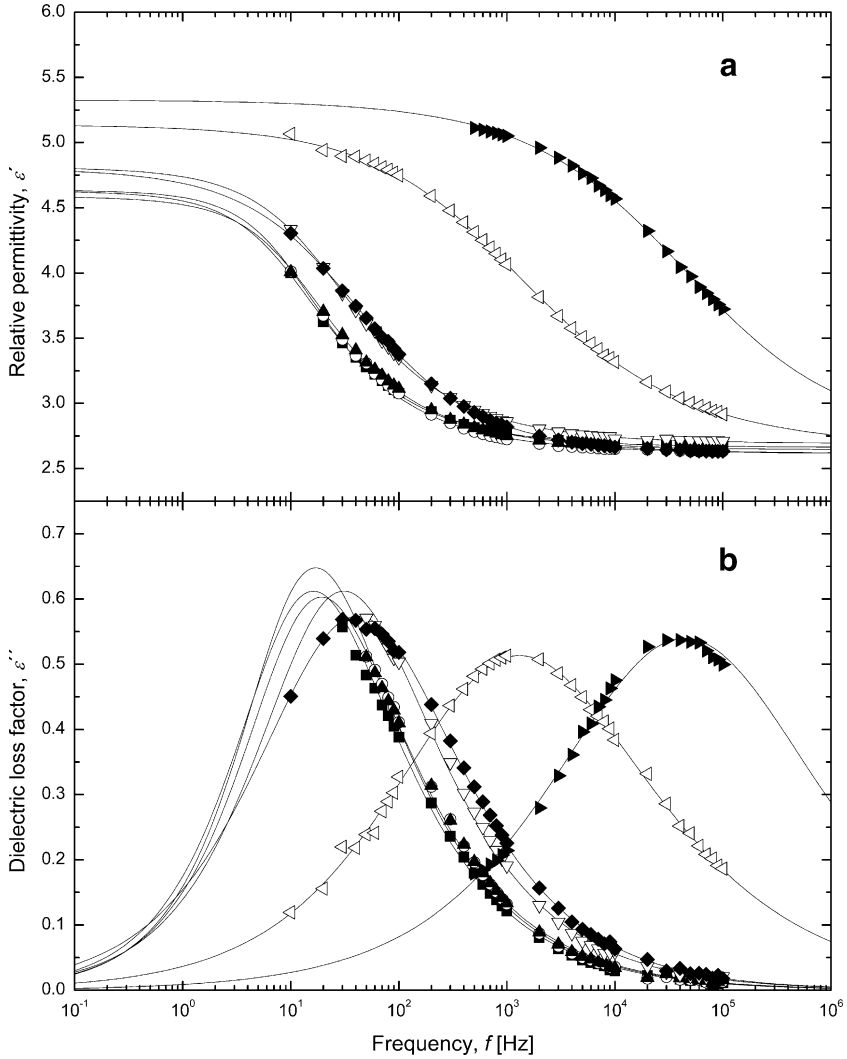

Fig. 4 Frequency spectra of relative permittivity ε' (**a**) and dielectric loss factor ε'' (**b**) for PANI suspensions protonated by tetrafluoroboric acid. Molar concentrations of acid C_A (mol l^{-1}) used for reprotonation of PANI base: ■ 0, ○ 0.0001, ▲ 0.0005, ▽ 0.001, ♦ 0.005, ◁ 0.01, ▶ 0.05. *Lines* are fits of the H–N model (Eq. 2)

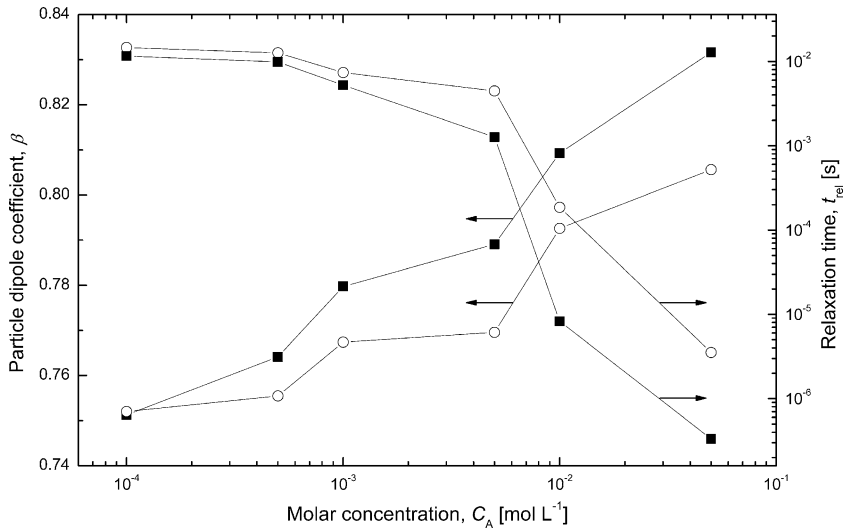

Fig. 5 The dependence of the particle dipole coefficient β and the relaxation time t_{rel} on molar concentration of acid, C_A. *Solid points*, *ortho*-phosphoric acid; *open points*, tetrafluoroboric acid

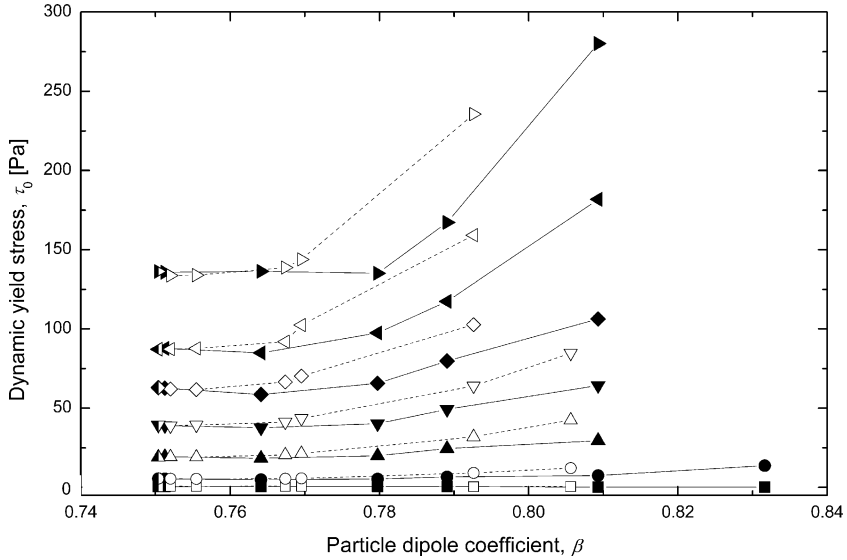

Fig. 6 The dependence of the dynamic yield stress τ_0 on the particle dipole coefficient β at various electric field strengths. *Points* denoted as in Fig. 2

Results and discussion

Electrorheological characterization The shear stress τ as a function of the shear rate $\dot{\gamma}$ was measured to characterize the ER behavior of PANI suspensions at seven various electric field strengths (0–3 kV mm^{-1}). Flow curves of the suspension of the sample P5 is presented as an example (Fig. 1). The field-off shear stress depends linearly on the shear rate and indicates a Newtonian flow. After electric field application, especially at low shear rates, the values of shear stress significantly rise by several orders of magnitude with increasing intensity of the electric field. The dynamic yield stresses τ_0 obtained by extrapolation of the shear stresses to the zero shear rate using the Herschel–Bulkley equation (Eq. 4) [28]:

$$\tau = \tau_0 + \eta_{\mathrm{pl}} \cdot \dot{\gamma}^n \tag{4}$$

(where η_{pl} is a plastic viscosity and n characterizes the pseudoplastic decrease in the viscosity of the system) indicate formation of the reinforced chain-like structures of organized polarized particles. A plateau region of the shear stresses appears at low shear rates due to the balance between electric and shear forces. At higher shear rates,

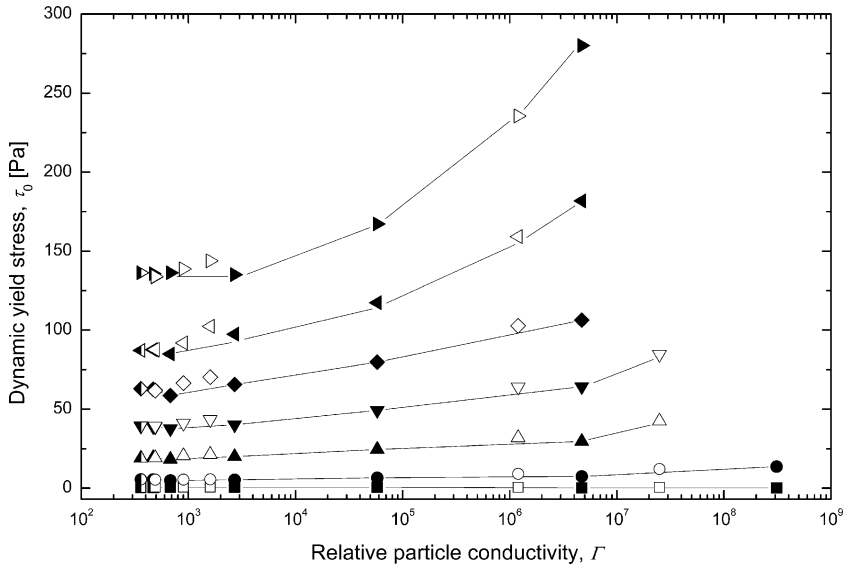

Fig. 7 The dependence of the dynamic yield stress τ_0 on the relative particle conductivity Γ ($=\sigma_p/\sigma_c$) at various electric field strengths. *Points* denoted as in Fig. 2

when the hydrodynamic forces begin to dominate over the electrostatic ones, these organized particle structures are gradually destroyed and the suspension tends to return to field-off Newtonian behavior.

The effect of PANI particle protonation The findings suggest that the doping level of the same concentration of various acids on particle polarization may vary. Thus, at constant electric field strength, the dynamic yield stress significantly depends not only on the protonation degree of PANI particles but also on the character of the acid used. At low protonation, τ_0 values achieve approximately similar constant values. At a higher protonation degree, the dynamic yield stresses of both suspensions of doped particles grew and diverged differently. In case of *ortho*-phosphoric acid at C_A=0.01 mol l^{-1} at the highest electric field strength used, τ_0 nearly doubled in value. For tetrafluoroboric acid, τ_0 was a little lower (Fig. 2). In samples doped to higher protonation at E>1.5 kV mm^{-1}, the current passing through the suspensions was too high; short circuit between electrodes sets in and the measurement failed. For example, the maximum current obtained for sample P5 was 2.1 mA, while for sample T5 it was only 0.20 mA.

Particle polarizability and relaxation time It is generally accepted that dielectric and conducting properties of suspension particles play important roles in the formation of ER structures and the general factors affecting this process are connected to particle polarizability. Thus, the forces between polarized particles and the rate at which polarization occurs are controlled by complex permittivity (Figs. 3 and 4). Until now, the results have shown that the main cause of the ER phenomenon is the interfacial polarization of suspended particles in the electric field, in

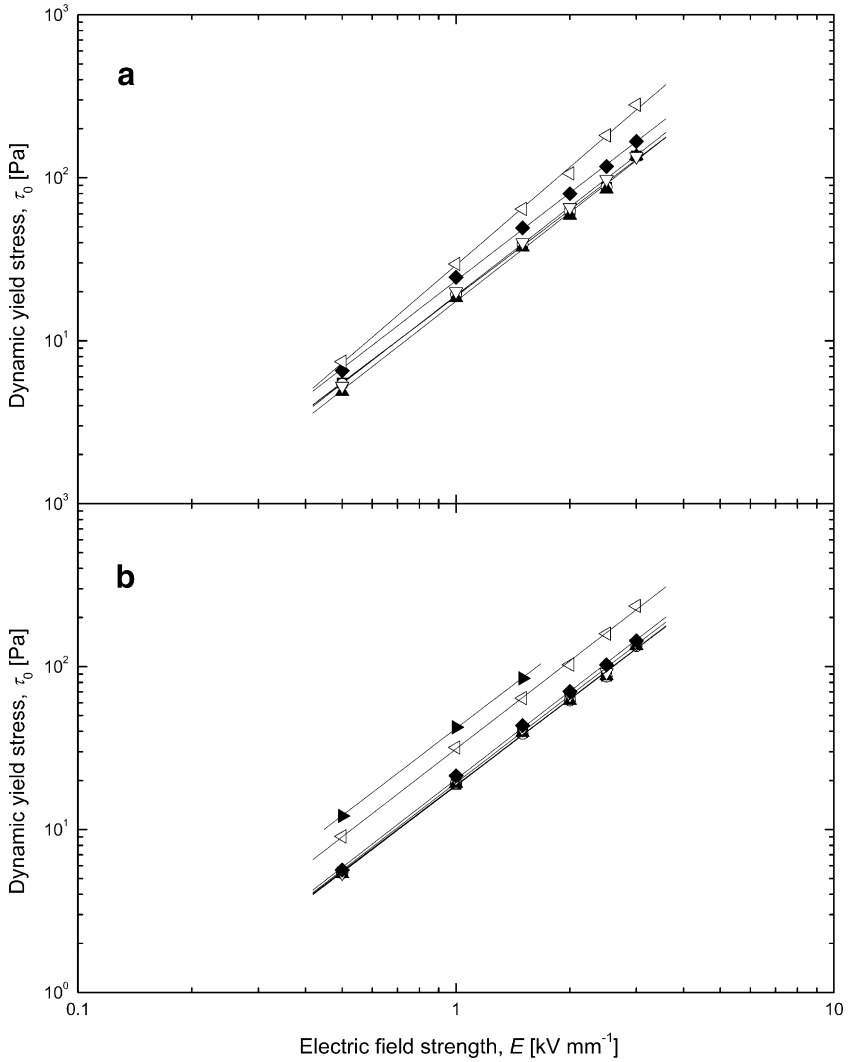

Fig. 8 The dependence of the dynamic yield stress τ_0 on the electric field strength E for PANI suspensions protonated by the *ortho*-phosphoric acid (**a**) and tetrafluoroboric acid (**b**). ■ P1/T1, ○ P2/T2, ▲ P3/T3, ▽ P4/T4, ♦ P5/T5, ◁ P6/T6, ▶ T7

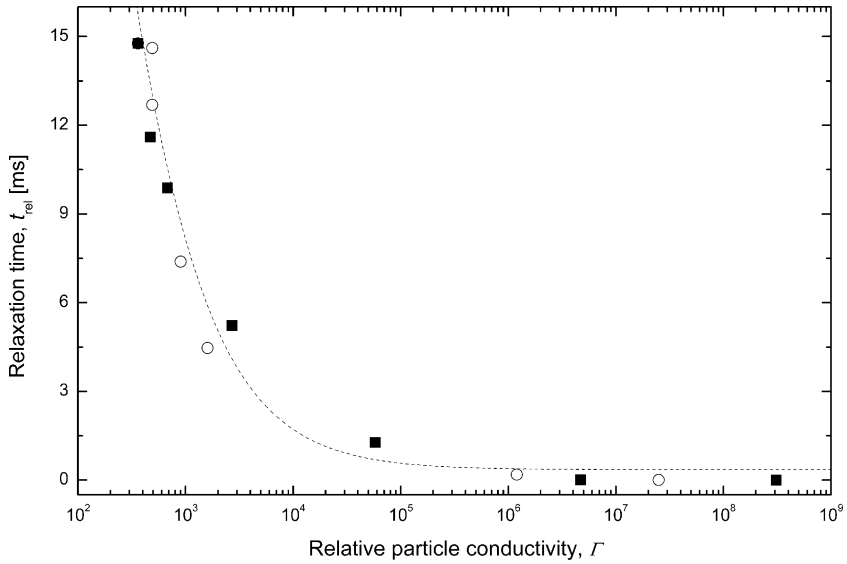

Fig. 9 The dependence of the relaxation time t_{rel} on the relative particle conductivity Γ ($=\sigma_p/\sigma_c$). *Points* denoted as in Fig. 5

which the relaxation frequency lies in the range $f=10^2$–10^5 Hz. The relaxation time t_{rel} (Eq. 5):

$$t_{rel} = 1/(2\pi f_{rel}) \tag{5}$$

depends on the relaxation frequency f_{rel} corresponding to the frequency at which the maximum dielectric loss factor $\varepsilon''_s(f)$ on the frequency spectrum appears. At the same time, the steepest decrease in permittivity arises.

According to the polarization models [28–35], a particle dipole coefficient β related to mismatch of particle permittivity and host fluid (Eq. 6):

$$\beta = \left(\varepsilon'_{p,0} - \varepsilon'_c\right) \Big/ \left(\varepsilon'_{p,0} + 2\varepsilon'_c\right) \tag{6}$$

is a general measure of particle polarizability.

The dielectric spectra demonstrate an increase in relative static permittivity $\varepsilon'_{p,0}$ and a steep decrease in relaxation time with particle protonation. The particle dipole coefficient β of particles doped with *ortho*-phosphoric acid (Tables 1 and 2) is higher and the relaxation time lower (Fig. 5) than those doped with tetrafluoroboric acid in the whole range of protonation, which suggests higher particle polarizability and faster reconstruction of the ER structure of polarized particles in the flow field.

Universal measures of ER efficiency The particle dipole coefficient β as a parameter controlling polarizability of PANI particles and rigidity of the ER structure has been investigated in the past. It appeared that correlation of the yield stress with β does not provide a common dependence for the suspensions of particles doped with *ortho*-phosphoric

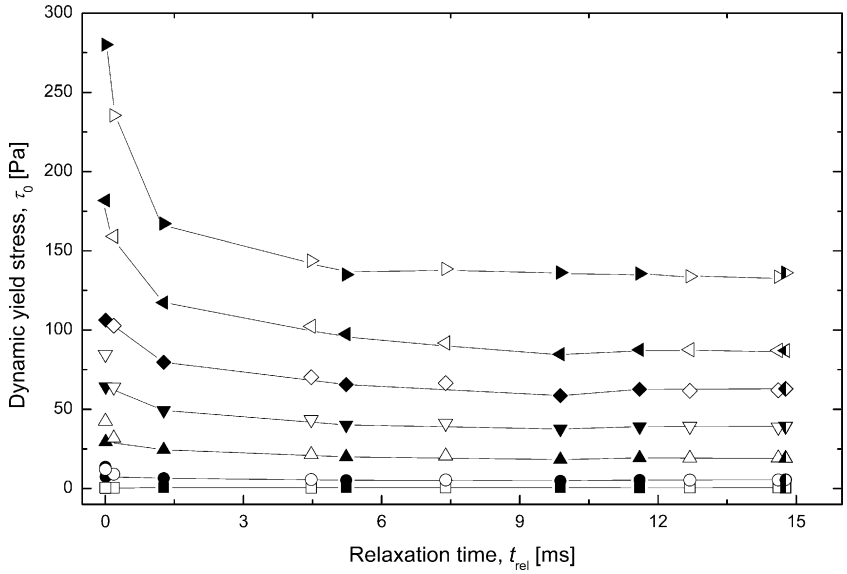

Fig. 10 The dependence of the dynamic yield stress τ_0 on the relaxation time t_{rel} at various electric field strengths. *Points* denoted as in Fig. 2

or tetrafluoroboric acid, especially at higher protonation degrees (Fig. 6). This means that particle permittivity is not a main factor affecting the ER behavior of materials under investigation. It may be assumed that, due to the high conductivity of particles, the ER efficiency could rather be controlled by the mismatch of conductivity of particles in the continuum [36–39]. The common dependence of the yield stress on the relative particle conductivity Γ as a ratio of conductivity of particles σ_p and that of continuum σ_c for PANI samples reprotonated with both acids (Fig. 7), and the slope of the log–log plot of the yield stress as a function of electric field strength 1.76–1.91 (Fig. 8) confirmed this assumption.

The relaxation time of both studied suspensions steeply decreased with the protonation degree of particles which indicates increasing particle mobility during restoration of the organized particle structure in the electric field. The common course of the correlations of the relaxation times with relative particle conductivity regardless of the way of protonation indicated a close connection between conductivity and particle mobility in the electric field (Fig. 9). As a consequence, the relaxation time, like particle conductivity, provided a common dependence of the yield stresses of ER suspensions irrespective of the acid used for protonation (Fig. 10).

Conclusions

The findings demonstrated that conductivity of PANI particles doped with various acids to higher protonation level, unlike particle permittivity, becomes the main factor controlling particle polarizability and may be a parameter integrating the dependences of the yield stress at various protonation degrees. In addition, the correlation of the yield stress with dielectric relaxation time relating to particle mobility during restoration of the ER structures in the electric field may provide a common course regardless the manner of protonation.

Acknowledgments The authors gratefully acknowledge the financial support from the Ministry of Education, Youth and Sports of the Czech Republic (MSM 7088352101) and the Grant Agency of the Czech Republic (202/06/0419).

References

1. Winslow WM (1947) US Patent 2 417 850
2. Block H, Kelly JP (1988) Electro-rheology. J Phys D Appl Phys 21:1661–1677
3. Jordan TC, Shaw MT (1989) Electrorheology. IEEE Trans Electron Insul 24:849–878
4. Block H, Kelly JP, Qin A, Watson T (1990) Materials and mechanisms in electrorheology. Langmuir 6:6–14
5. Parthasarathy M, Klingenberg DJ (1996) Electrorheology: mechanisms and models. Mater Sci Eng R 17:57–103
6. Hao T (2001) Electrorheological fluids. Adv Mater 13:1847–1857
7. Hao T (2002) Electrorheological suspensions. Adv Colloid Interface Sci 97:1–35
8. See H (1999) Advances in modelling the mechanisms and rheology of electrorheological fluids. Korea–Austr Rheol J 11:169–195
9. Papadopulous CA (1998) Brakes and clutches using ER fluids. Mechatronics 8:719–726
10. Quadrat O, Stejskal J (2006) Polyaniline in electrorheology. J Ind Eng Chem 12:352–361
11. Choi HJ, Lee JH, Cho MS, Jhon MS (1999) Electrorheological characterization of semiconducting polyaniline suspension. Polym Eng Sci 39:493–499
12. Pavlínek V, Sáha P, Kitano T, Stejskal J, Quadrat O (2005) The effect of polyaniline layer deposited on silica particles on electrorheological and dielectric properties of their silicone-oil suspensions. Physica A 353:21–28
13. Sung JH, Cho MS, Choi HJ, Jhon MS (2004) Electrorheology of semiconducting polymers. J Ind Eng Chem 10:1217–1229
14. Cheng Q, Pavlínek V, Lengálová A, Li Ch, Belza T, Sáha P (2006) Electrorheological properties of new mesoporous material with conducting polypyrrole in mesoporous silica. Micropor Mesopor Mater 94:193–199
15. Chin BD, Lee YS, Park OO (1998) Effects of conductivity and dielectric behaviours on the electrorheological response of a semiconductive poly(*p*-phenylene) suspension. J Colloid Interface Sci 201:172–179
16. Plocharski J, Rozanski M, Wycislik H (1999) Electrorheological effect in suspensions of conductive polymers. Synth Met 102:1354–1357
17. Stejskal J, Kratochvíl P, Jenkins AD (1996) The formation of polyaniline and the nature of its structures. Polymer 37:367–369
18. Lee JH, Cho MS, Choi HJ, Jhon MS (1999) Effect of polymerization on the temperature polyaniline based electrorheological suspensions. Colloid Polym Sci 277:73–76
19. Jang WH, Kim JW, Choi HJ, Jhon MS (2001) Synthesis and electrorheology of camphorsulfonic acid doped polyaniline suspensions. Colloid Polym Sci 279:823–827
20. Hong CH, Choi HJ (2007) Shear stress and dielectric analysis of H_3PO_4 doped polyaniline based electrorheological fluid. J Macromol Sci B Phys 46:683–692
21. Chaudhari HK, Kelkar DS (1997) Investigation of structure and electrical conductivity in doped polyaniline. Polym Int 42:380–384
22. Chandrasekhar P (1999) Conducting polymers, fundaments and applications. Kluwer, Boston
23. Stěnička M, Pavlínek V, Sáha P, Blinova NV, Stejskal J, Quadrat O (2008) Conductivity of flowing polyaniline suspensions in electric field. Colloid Polym Sci 286(12):1403–1409. doi:10.1007/s00396-008-1910-2
24. Blinova NV, Stejskal J, Trchová M, Prokeš J (2008) Control of polyaniline conductivity and contact angles by partial protonation. Polym Int 57:66–69
25. Stejskal J, Gilbert RG (2002) Polyaniline. Preparation of a conducting polymer (IUPAC technical report). Pure Appl Chem 74:857–867
26. Havriliak S Jr, Havriliak SJ (1997) Dielectric and mechanical relaxation in materials. Hanser, Munich
27. Marshall L, Zukoski CF IV, Goodwin JW (1989) Effects of electric fields on the rheology of non-aqueous concentrated suspensions. J Chem Soc Faraday Trans 85:2785–2795
28. Herschel WH, Bulkley R (1926) Konsistenzmessungen von Gummi-Benzol-Lösungen. Kolloid Z 39:291–300

29. Gast AP, Zukoski CF (1989) Electrorheological fluids as colloidal suspensions. Adv Colloid Interface Sci 30:153–170
30. Klingenberg DJ, Zukoski CF (1990) Studies on the steady-shear behaviour of electrorheological suspensions. Langmuir 6:15–24
31. Halsey TC, Toor W (1990) Structure of electrorheological fluids. Phys Rev Lett 65:2820–2823
32. Block H, Kelly JP, Qin A, Watson T (1990) Materials and mechanisms in electrorheology. Langmuir 6:6–14
33. Chen Y, Sprecher AF (1991) Electrostatic particle–particle interactions in electrorheological fluids. J Appl Phys 70:6796–6803
34. Davis LC (1992) Finite-element analysis of particle–particle forces in electrorheological fluids. Appl Phys Lett 60:319–321
35. Ikazaki F, Kawai A, Uchida K, Kawakami T, Edmura K, Sakurai K, Anzai H, Asako Y (1998) Mechanisms of electrorheology: the effect of the dielectric property. J Phys D Appl Phys 31:336–347
36. Anderson RA (1992) Effects of finite conductivity in electrorheological fluids. In: Tao R (ed) Proceedings of the 3rd International Conference on Electromagnetic Fluids. World Scientific, Singapore, pp 81–90
37. Davis LC (1992) Polarization forces and conductivity effects in electrorheological fluids. J Appl Phys 72:1334–1340
38. Tang X, Wu CW, Conrad H (1995) On the conductivity model for the electrorheological effect. J Rheol 39:1059–1073
39. Wu CW, Conrad H (1996) A modified conduction model for the electrorheological effect. J Phys D Appl Phys 29:3147–3153